Mucosal Adaptation to Enteral Nutrients Is Dependent on the Physiologic Actions of Glucagon-Like Peptide-2 in Mice

ERIC D. SHIN,* JENNIFER L. ESTALL,† ANGELO IZZO,* DANIEL J. DRUCKER,†,§,‖ and PATRICIA L. BRUBAKER*,§

Departments of *Physiology, †Laboratory Medicine and Pathobiology, and §Medicine, and the ‖Banting and Best Diabetes Centre, University of Toronto, Toronto, Ontario, Canada

Background & Aims: **Our understanding of the intestinotropic actions of glucagon-like peptide-2 (GLP-2)$^{1–33}$ is based on pharmacologic studies involving exogenous administration. However, the physiologic role of GLP-2 in mucosal growth and adaptation to nutritional stimulation remains poorly understood.** ***Methods:*** **The properties of GLP-2$^{3–33}$, a GLP-2$^{1–33}$ metabolite, were determined in baby-hamster kidney cells transfected with the mouse GLP-2 receptor complementary DNA and in isolated murine intestinal muscle strips. To investigate the role of endogenous GLP-2$^{1–33}$ in gut adaptation, GLP-2$^{3–33}$ was administered to mice that were re-fed for 24 hours after 24 hours of fasting, and the small intestine was analyzed. GLP-2$^{3–33}$ also was injected into rats for analysis of circulating GLP-2$^{1–33}$ levels.** ***Results:*** **GLP-2$^{3–33}$ antagonized the actions of GLP-2$^{1–33}$ in vitro and ex vivo. Fasting mice exhibited small intestinal atrophy (37% ± 1% decrease in small intestinal weight, 19% ± 2% decrease in crypt-villus height, and 99% ± 35% increase in villus apoptosis, $P < .05–.01$). Adaptive growth in re-fed mice restored all these parameters, as well as crypt-cell proliferation, to normal control levels ($P < .05$ vs. fasting); these adaptive changes were prevented partially or completely by co-administration of GLP-2$^{3–33}$ to refeeding mice (by 32% ± 19% to 103% ± 15%, $P < .05–.01$ vs re-fed mice). Exogenous GLP-2$^{3–33}$ did not affect endogenous GLP-2$^{1–33}$ levels.** ***Conclusions:*** **These data show that endogenous GLP-2 regulates the intestinotropic response in re-fed mice through modulation of crypt-cell proliferation and villus apoptosis. GLP-2 is therefore a physiologic regulator of the dynamic adaptation of the gut mucosal epithelium in response to luminal nutrients.**

The small intestine exhibits a remarkable capacity to adapt to changes in nutritional status whereby the absence of luminal nutrients induces mucosal atrophy, and subsequent reintroduction of enteral nutrition results in adaptive regrowth of the mucosal epithelium.[1,2] Although most species exhibit some degree of gut adaptation in response to a nutrient challenge,[3,4] the murine fasting and refeeding model shows exceptional plasticity within a very short time frame. Mice that undergo fasting for 24 hours exhibit significant atrophy of the gut, whereas refeeding for a subsequent 24 hours restores the gut epithelium toward normal.[1] This atrophy and subsequent regrowth are associated with decreased and increased crypt-villus height, respectively. A number of different hormones have been implicated in regulating gut growth including insulin-like growth factor-1, growth hormone, keratinocyte growth factor, and epidermal growth factor.[5] More recently, interest has focused on the actions of the intestinal hormone glucagon-like peptide-2 (GLP-2) not only because of its potent intestinotropic effects, but also because of the pleiotropic effects of GLP-2 on nutrient absorption, gut permeability, and mucosal cytoprotection.[6,7]

GLP-2 is a 33 amino-acid peptide secreted by the enteroendocrine L cell of the intestinal epithelium.[8–10] Exogenous administration of GLP-2 to normal rodents, as well as to rodents with intestinal damage or inflammation, stimulates intestinal epithelial growth through increased proliferation in the crypts and decreased apoptosis in the villus tips.[6,7,11–14] Exogenous GLP-2 administration also increases nutrient absorption, decreases intestinal permeability, and inhibits gastrointestinal motility.[15–19] Consistent with these findings, preclinical studies in patients with short-bowel syndrome showed that administration of GLP-2 increased their capacity to absorb enteral nutrients.[20]

Circulating levels of GLP-2 are decreased in the fasting state. GLP-2 secretion from the L cell is stimulated by ingestion of nutrients, specifically carbohydrates and

Abbreviations used in this paper: DP-IV, dipeptidylpeptidase-IV; EC_{50}, median effective concentration; GLP-2, glucagon-like peptide-2; HPLC, high-performance liquid chromatography; h, human; m, mouse; PCR, polymerase chain reaction; r, rat; RT, reverse transcription; TUNEL, terminal deoxynucleotide transferase–mediated deoxyuridine triphosphate nick-end labeling.

0016-5085/05/$30.00
doi:10.1053/j.gastro.2005.02.033

Table 1. GLP-2 Sequences

Species	Mouse homology	1 2	3 4 5	6 7 8 9 10	11 12 13 14 15	16 17 18 19 20	21 22 23 24 25	26 27 28 29 30	31 32 33
Mouse	–	HA	DGS	FSDEM	STILD	NLATR	DFINW	LIQTK	ITD
Rat	97%	HA	DGS	FSDEM	NTILD	NLATR	DFINW	LIQTK	ITD
Human	94%	HA	DGS	FSDEM	NTILD	NLAAR	DFINW	LIQTK	ITD
Human (Gly^2)-GLP-2	91%	HG	DGS	FSDEM	NTILD	NLAAR	DFINW	LIQTK	ITD

NOTE. Residues highlighted in black are different from the mouse sequence. Underlined residues represent the dipeptide that is removed by DP-IV to produce the corresponding GLP-2^{3-33}.

fat.[9,10,21] The plasma half-life of exogenously administered GLP-2 is approximately 7 minutes in humans,[22] caused in part by renal clearance and enzymatic inactivation of the full-length peptide by the ubiquitous enzyme dipeptidylpeptidase-IV (DP-IV). DP-IV cleaves 2 amino acids off the N-terminal end of GLP-2^{1-33}, liberating the metabolite, GLP-2^{3-33}.[23,24] Although GLP-2^{3-33} has been shown to be inactive biologically with respect to the stimulation of intestinal growth,[23,25] GLP-2^{3-33} has been shown to function both as a weak partial agonist and as an antagonist when given together with exogenous GLP-2^{1-33} in mice.[26]

Our current understanding of GLP-2 as an intestinotropic hormone has been based largely on pharmacologic studies in which the peptide has been administered exogenously, leading to supraphysiologic levels of circulating GLP-2. In contrast, the lack of well-characterized GLP-2–receptor (GLP-2R) antagonists has constrained our understanding of the physiologic role of endogenous GLP-2 under different experimental conditions. In the current study we cloned the mouse GLP-2R complementary DNA (cDNA) and used this reagent, as well as an ex vivo mouse muscle strip preparation, to show that GLP-2^{3-33} is a murine GLP-2R antagonist. Furthermore, we used GLP-2^{3-33} to test the hypothesis that endogenous GLP-2^{1-33} is required for nutrient regulation of intestinal mucosal growth.

Materials and Methods

Peptides

Synthetic rat (r) GLP-2^{3-33} and rGLP-2^{5-33} were provided by NPS-Allelix Biopharmaceuticals (Mississauga, Ontario, Canada). Human (h) GLP-2^{3-33} was purchased from Peptidec Technologies, Ltd. (Pierrefonds, Quebec, Canada), and the degradation-resistant analog h(Gly^2)-GLP-2^{1-33} was obtained from American Peptide Company (Sunnyvale, CA). The various molecular forms of GLP-2 used in this study have a high sequence homology, as shown in Table 1. The authenticity and integrity of these peptides were verified by mass spectrometry (data not shown, University of Toronto, Toronto, Ontario, Canada). Synthetic GLP-$1^{7-36NH2}$ was purchased from Bachem California, Inc. (Torrance, CA) and rat albumin was purchased from Sigma Chemical Co. (St. Louis, MO).

Animals

Six-week-old female CD1 mice and 400–500 g adult male Wistar rats were obtained from Charles River Canada (St. Constant, Quebec, Canada). All animal protocols were approved by the Animal Care Committee of the University of Toronto.

Reverse-Transcription Polymerase Chain Reaction Amplification of Mouse GLP-2R mRNA and cDNA Cloning

Total cellular RNA was extracted from colon and jejunum of mice (C57BL/6) with Trizol reagent (Invitrogen Life Technologies, Inc, Burlington, Ontario, Canada). A total of 10–12 μg of RNA from each tissue was treated with deoxyribonuclease I and reverse transcribed using random hexamers and the Superscript II first-strand synthesis kit (Invitrogen Life Technologies, Inc.), according to the manufacturer's instructions. To control for contamination, reactions also were performed in the absence of Superscript II. First-strand cDNAs were treated with ribonuclease H to remove RNA, and polymerase chain reactions (PCRs) were performed using *Taq* DNA polymerase (MBI Fermentas, Burlington, Ontario, Canada) with first-strand cDNAs as templates. Sense (5′-AGGGGTACCGCCACCATGCGTCGGCTCTGGGGCCCT-3′) and antisense (5′-TTAGATCTCACTCTCTTCCAGAATCTC-3′) primers (ACTG, Toronto, Ontario, Canada) were used for 45 cycles of PCR performed at 95°C for 1 minute, 65°C for 2 minutes, and 72°C for 1.5 minutes. The sense primer was designed to insert a *Kpn* I site and an optimized Kozak sequence upstream of the initiator start codon. To verify specificity of the PCR product, aliquots from each reaction were resolved by gel electrophoresis and transferred to a nylon membrane (Schleicher & Schuell Bioscience, Keene, NH). The identity of the 1.6-kb full-length mouse (m) GLP-2R cDNA was confirmed after hybridization to a [^{32}P]-labeled internal cDNA fragment of the rGLP-2R, as described previously.[25,27]

Aliquots of colon and jejunum PCR reactions were purified on GFX PCR columns (Amersham Biosciences, Piscataway, NJ) and ligated to the pCR4 vector using the Topo TA cloning kit (Invitrogen Life Technologies). GLP-2R cDNA clones from both jejunum and colon were isolated and full-length mGLP-2R cDNA was sequenced (Core Molecular Biology Facility, York University, Ontario, Canada), and ligated into the *Kpn* I and *Eco* RI sites of pcDNA 3.1 (Invitrogen Life Technologies, Inc.) for expression studies. Because the GLP-2R

cDNA sequences from mouse jejunum and colon were identical, further studies were performed using the GLP-2 receptor cDNA cloned from the jejunum.

In Vitro Studies

Baby-hamster kidney (BHK) fibroblasts were transfected transiently with the mouse GLP-2R cDNA (BHK-mGLP-2R) using FuGene (Roche Diagnostics, Quebec, Canada). Cells were plated in standard tissue culture dishes and grown in Dulbecco's modified Eagle medium with high glucose (4.5 g/L) and 10% fetal bovine serum at 37°C with 5% CO_2 and constant humidity. Twenty-four hours after transfection, GLP-2R activation was assessed by measuring adenosine 3′,5′-cyclic monophosphate (cAMP) production, as previously described.[25,28] In brief, all treatments were prepared in Dulbecco's modified Eagle medium containing 100 μmol/L 3-isobutyl-1-methylxanthine. Cells were preincubated for 5 minutes at 37°C in medium containing vehicle or rGLP-2^{3-33} before the addition of media alone (basal), rGLP-2^{3-33}, and/or h(Gly^2)-GLP-2 at the indicated concentrations for 10 minutes. The reaction was terminated by addition of 1 mL of anhydrous ethyl alcohol at −20°C (final concentration, 77% EtOH) and plates were allowed to sit at −20°C for 24 hours. The extracts were collected and cAMP levels were determined by using a cAMP radioimmunoassay kit (Biomedical Technologies, Stoughton, MA). cAMP levels were normalized to total cellular protein, as determined by using the Bradford assay (Bio-Rad Laboratories, Hercules, CA). Basal cAMP levels were .33 ± .01 pmole/μg protein, and 100 μmol/L forskolin (positive control) increased cAMP production by 381% ± 50% ($P < .01$).

Ex Vivo Studies

One-centimeter sections of midjejunum (collected between 16–24 cm distal to the pyloric sphincter) were excised from female CD1 mice that were euthanized by cervical dislocation. Muscle layers then were stripped from the mucosa and analyzed for GLP-2R mRNA transcripts by reverse-transcription (RT)-PCR, as described below, or collected in ice-cold Hanks' balanced salt solution. All treatments were prepared in Dulbecco's modified Eagle medium with low glucose (1.0 g/L) containing 50 μmol/L 3-isobutyl-1-methylxanthine. Each treatment group contained two 1-cm muscle strips and were preincubated for 5 minutes at room temperature in media containing vehicle or GLP-2^{3-33} before a 30-minute incubation with media alone (control), GLP-2^{3-33}, and/or h(Gly^2)-GLP-2 at the indicated concentrations at 37°C with 5% CO_2. The reaction was terminated by homogenization of the muscle strips with ethanol at −20°C, followed by centrifugation to remove the debris. The supernatant then was assayed for cAMP while the pellet was dissolved in 80% formic acid and assayed for protein, as described earlier. Basal cAMP levels for muscle strip experiments were .0169 ± .0013 pmol/μg protein.

In Vivo Studies

Mice had free access to water but access to standard chow was determined by their respective treatments. Fasted mice had no access to chow for the 24-hour period before they were killed. Re-fed mice were fasted for 24 hours followed by a 24-hour refeeding period. Vehicle (phosphate-buffered saline [PBS]), rGLP-2^{3-33} (.3, 1, 3, or 30 ng), hGLP-2^{3-33} (3 or 30 ng), rGLP-2^{5-33} (30 ng), GLP-1 (30 ng), or rat albumin (660 ng; molar equivalent to 30 ng of GLP-2^{3-33}) was administered subcutaneously 24 and 12 hours before death. In re-fed mice, vehicle or peptide administration coincided with the 24-hour refeeding period.

Small intestines were collected from euthanized mice and the weights were determined after gentle removal of the luminal contents and the mesenteric fat. The proximal duodenum (first 5 cm immediately after the pyloric sphincter) was homogenized in 2.4 mL of PBS and stored at −20°C until assessment of enzymatic activity. A 5-cm distal duodenal section (8–13 cm distal to the pyloric sphincter) was collected to determine water and protein composition. A 1-cm segment from the proximal jejunum (13–14 cm distal to the pyloric sphincter) was divided into 4 cross-sections, fixed in 10% neutral-buffered formalin, paraffin embedded, and cut into 4-μm sections for morphometry and immunohistochemistry. One-centimeter sections from jejunum and ileum (16–17 cm distal to the pyloric sphincter and 2–3 cm proximal to the cecum, respectively) also were excised, snap-frozen in liquid nitrogen, and stored at −80°C for RT-PCR.

Morphometry and Immunohistochemistry

Morphometric analysis was performed on cross-sections stained with H&E using a Zeiss microscope with Axio Vision Software (Carl Zeiss Canada, Don Mills, Ontario, Canada). For each mouse, the mean crypt-villus height was obtained from blinded measurements made in all 4 cross-sections, with an average of 28 measurements made for each mouse.

Immunohistochemistry for Ki-67, a marker expressed exclusively during proliferative stages of the cell cycle,[29] was performed using the rat anti-mouse Ki-67 TEC-3 antibody (DAKO, Glostrup, Denmark). In brief, endogenous peroxidase activity was blocked with 3% H_2O_2 and, after antigen retrieval, nonspecific binding was blocked with Blocking Reagent (Signet, Dedham, MA). The primary antibody was applied at a dilution of 1:150 for 1 hour at room temperature, followed by rabbit biotinylated anti-rat immunoglobulin G antibody (1:200; Vector, Burlingame, CA) for 30 minutes at room temperature. Visualization was performed using Ultra Streptavidin–Horseradish Peroxidase Complex: Level 2 Labeling Reagent (Signet) with 3,3′-diaminobenzidine (Vector), followed by counterstaining with hematoxylin (Sigma Chemical Company). For negative controls, the primary antibody was omitted from the protocol. For each mouse an average of 25 well-oriented and intact half crypts were analyzed. For each half crypt, 20 cells were counted with the cell at the base of the crypt designated as position 0. Proliferation was determined by counting the number of labeled cells relative to total cells for every cell position.

Table 2. Primer Sequences Used for RT-PCR

Primers	Sequence	Product size	Melting temperature	Cycle number	References
Proglucagon	F: 5′-TGAAGACCATTTACTTTGTGGCT-3′ R: 5′-TGGTGGCAAGATTGTCCAGAAT-3′	492 bp	60°C	30	(32)
GLP-2R	F: 5′-TCATCTCCCTCTTCTTGGCTCTTAC-3′ R: 5′-TCTGACAGATATGACATCCATCCAC-3′	196 bp	60°C	29	(30)
18S rRNA	F: 5′-TCAAGAACGAAAGTCGGAGG-3′ R: 5′-GGACATCTAAGGGCATCACA-3′	488 bp	60°C	19	(31)

F, forward primer; R, reverse primer; rRNA, ribosomal RNA.

Apoptosis was assessed by detection of DNA fragmentation using an in situ terminal deoxynucleotide transferase–mediated deoxyuridine triphosphate nick-end labeling (TUNEL) assay. Sections were processed with an ApopTag in situ Apoptosis Detection Kit (Intergen, Purchase, NY) according to the manufacturer's instructions. Rat mammary gland tissue provided in the kit was used as a positive control, and terminal deoxynucleotide transferase enzyme was omitted from the reaction mixture for the negative control. Apoptosis initially was determined for the entire length of the crypt-villus axis. However, pilot studies determined that the majority of apoptotic cells resided in the first 30 cell positions from the villus tip (position 0; data not shown). The occurrence and position of apoptotic cells therefore were recorded along the villus axis for the first 30 cells of 50 well-oriented and intact half villi (on average) for each mouse.

Biochemical Analyses

To determine small intestinal composition, tissue samples were weighed (wet weight) and then frozen at −80°C before being lyophilized and weighed again (dry weight). The H_2O contribution to total weight was determined by subtracting the dry weight from the wet weight. The dried tissue then was reconstituted in 5 mL of distilled H_2O and homogenized and the protein content was determined by Bradford assay (Bio-Rad Laboratories).

Frozen duodenal sections were homogenized in 2.4 mL of sodium phosphate buffer, pH 7, at 4°C for determination of maltase, sucrase, and DP-IV activity, as previously described.[15] Activity of all enzymes was expressed per gram of protein, and 1 unit of activity (U) represents 1 μmol of substrate hydrolyzed/min at 37°C.

RT-PCR

Total tissue RNA was extracted using the RNeasy kit (Qiagen, Mississauga, Ontario, Canada), with RNase-free DNase-I (Qiagen). Total RNA levels were quantified for each tissue using ultraviolet absorbance at 260 nm. Oligonucleotide primers for semiquantitative RT-PCR are shown in Table 2.[30–32]

Semiquantitative RT-PCR was performed using the One-Step RT-PCR kit (Qiagen) according to the manufacturer's instructions. Proglucagon RT-PCR conditions were as follows: 50°C for 30 minutes, and 95°C for 15 minutes, followed by 94°C for 1 minute, 67°C for 1 minute, and 72°C for 1 minute for 30 cycles, and then by 72°C for 10 minutes. GLP-2R and RT-PCR conditions were as follows: 50°C for 30 minutes, 95°C for 15 minutes, followed by 94°C for 1 minute, 57.8°C for 1 minute, and 72°C for 1 minute for 29 cycles, and then by 72°C for 10 minutes. The 18S ribosomal RNA RT-PCR conditions were as follows: 50°C for 30 minutes, and 95°C for 15 minutes, followed by 94°C for 1 minute, 60°C for 45 seconds, and 72°C for 1 minute for 19 cycles, and then 72°C for 10 minutes. RT-PCR product sizes were verified on a 1.5% agarose gel electrophoresis stained with ethidium bromide and a parallel reaction with omission of the reverse-transcriptase enzyme was performed to show the absence of contaminating genomic DNA (data not shown). RT-PCR products were quantified by ion-exchange high-performance liquid chromatography (HPLC) analysis. Briefly, HPLC was performed using a Waters Breeze system (Waters Ltd, Mississauga, Ontario, Canada) with a TSK-GEL DNA-NPR column (4.6 mm × 75 mm; TOSOH Bioscience, Montgomeryville, PA). Eluant A (20 mmol/L Tris, pH 9.0) and eluant B (1 mol/L NaCl and 20 mmol/L Tris, pH 9.0) were used for gradient elution, as follows: 53.5% eluant B for 1 minute, then a linear increase to 58.5% eluant B for 2 minutes, followed by another increase to 100% eluant B for .3 minutes, and a purge at 100% eluant B for 1.7 minutes, all at 1 mL/min. Areas of the proglucagon and GLP-2R RT-PCR products (as detected at 254 nm) were normalized to those of the 18S product. Linear RT-PCR amplification was determined using a range of input total RNA concentrations and different cycle numbers (data not shown).

Plasma GLP-2 Levels

Analysis of both GLP-$2^{1–33}$ and GLP-$2^{3–33}$ was performed using HPLC and radioimmunoassay, as previously described.[21] These studies were performed in rats because extensive analyses using murine samples showed high levels of variation as a consequence of the requirement for pooling of plasma from up to 7 animals to make each n = 1. Briefly, rats were anesthetized lightly by using halothane before receiving a 60 mg/kg intraperitoneal injection of sodium pentobarbital. Blood samples were collected 30 minutes after subcutaneous injection of either PBS (vehicle) or GLP-$2^{3–33}$ (1.2 μg/kg, equivalent to the 30-ng dose of GLP-$2^{3–33}$ administered to mice). Blood samples (7 mL) were collected into 700 μL Trasylol (5000 kallikrein inactivating units/mL; Bayer, Inc, Toronto, Ontario, Canada), ethylenediaminetetraacetic acid (1.2 mg/mL), and diprotin-A (.1 mmol/L). Plasma then was

separated from red blood cells by centrifugation, followed by extraction of peptides from 2 mL of plasma by addition of 4 mL 1% trifluoroacetic acid (pH adjusted to 2.5 with diethylamine) and collection on a C_{18} Sep Pak cartridge (Waters Associates, Bedford, MA). GLP-2^{1-33} and GLP-2^{3-33} were separated by HPLC on a C_{18} μBondapak column (Waters Associates); the gradient conditions were: 10%–40% solvent B over 20 minutes and then 40%–50% solvent B over 20 minutes, followed by a purge with 99% solvent B for 10 minutes (solvent A = .1% trifluoroacetic acid in water and solvent B = .1% trifluoroacetic acid in acetonitrile), at a flow rate of 1 mL/min. Fractions were collected at .3-minute intervals, dried, and analyzed by radioimmunoassay for GLP-2 using the midsequence-directed antiserum, UTTH-7, as previously described.[21] All data are normalized to the peak value of GLP-2^{1-33}, corresponding to the elution position of synthetic GLP-2^{1-33}.

Data Analysis

All data are expressed as mean ± SE. The median effective concentration (EC_{50}) was calculated using GraphPad Prism software (GraphPad Software, San Diego, CA). Area-under-the-curve for GLP-2 HPLC peaks was determined using the trapezoidal method. Statistical significance was established by the Student *t* test or analysis of variance with n-1 custom hypotheses post hoc tests, as appropriate, using SAS (Statistical Analysis Systems, Cary, NC) software. Statistical significance was defined as $P \leq .05$.

Results

Cloning of the mGLP-2R

To clone the mGLP-2R cDNA, we used a combination of RT-PCR and hybridization screening. Amplification of first-stand mRNA from either mouse jejunum or colon was performed with primers designed to be complementary to the published sequences from the 5′ end of the mGLP-2R (GenBank Accession number AF338224) and the 3′ end of a published mouse cDNA clone (GenBank NM175681) and yielded a PCR product approximately 1.6 kb in length. Hybridization of a Southern blot with an internal oligonucleotide probe complementary to GLP-2R sequences verified the specificity of the PCR product, as described in the Materials and Methods section. Sequencing and comparison of multiple cDNA clones isolated from preparations of RNA from jejunum and colon yielded identical nucleotide sequences corresponding to a single cDNA (GenBank AY605231) encoding the full-length mGLP-2R (Figure 1). The cloned mGLP-2R cDNA (GenBank AY605231) differs from a previously published clone, originally isolated as part of a full-length mouse cDNA library (GenBank NM175681), at 4 amino acids (P263H, G459A, V460F, and R485L). Our mGLP-2R amino acid sequence shows 85%–90% identity with the published human and rat GLP-2R sequences, respectively (GenBank AF105367 and AF105368), with highest similarities in the regions encoding the N-terminus, the transmembrane segments, and the distal C-terminus. Functional analysis of the transfected receptor cDNA was performed after subcloning of the mGLP-2R cDNA into an expression vector (pcDNA 3.1).

Characterization of the Function of GLP-2^{3-33} at the Murine GLP-2 Receptor

To determine whether rGLP-2^{3-33} can antagonize the effects of h(Gly^2)-GLP-2 on the mGLP-2R, levels of cAMP were examined in BHK cells treated with various peptides after transient transfection with the mGLP-2R. h(Gly^2)-GLP-2 dose-dependently stimulated BHK mGLP-2R cAMP production with an EC_{50} of .40 nmol/L (95% confidence interval, .16–1.04 nmol/L) (Figure 2*A*). Preincubation with 100–1000 nmol/L rGLP-2^{3-33} significantly shifted the dose-response curve, with an EC_{50} of 1.63 nmol/L (.77–3.47 nmol/L, $P < .05$) and 52.89 nmol/L (16.62–168.3 nmol/L, $P < .05$), respectively (Figure 2*A*). However, the maximal response (.95 ± .03 pmol/μg) was not significantly different for h(Gly^2)GLP-2 with or without rGLP-2^{3-33}. Together, these data suggest that rGLP-2^{3-33} is acting as a competitive antagonist on the transfected mouse GLP-2R. Furthermore, rGLP-2^{3-33} alone exerted a partial agonist effect, with an EC_{50} of 929.7 nmol/L (44.91–19,246 nmol/L) and a maximal response that was 37% ± 2% of that seen for h(Gly^2)-GLP-2 (Figure 2*A*).

To assess whether GLP-2^{3-33} also antagonizes GLP-2 action in a separate independent experimental model, a novel ex vivo murine intestinal muscle strip preparation was developed. RT-PCR analysis confirmed the presence of mRNA transcripts for the GLP-2R in the isolated muscle strips, and addition of h(Gly^2)GLP-2 stimulated cAMP production, with a maximal response of 234% ± 79% of controls at 10^{-10} mol/L (Figure 2*B*, *C*). Higher doses of h(Gly^2)GLP-2 showed reduced cAMP responses, consistent with previous reports.[33–35] GLP-2^{3-33} (10^{-8} mol/L) alone did not stimulate cAMP production (110% ± 11%, of controls, $P > .05$) but completely attenuated the stimulatory effect of GLP-2^{1-33} ($P < .05$) (Figure 2*D*). These experiments strongly suggest that GLP-2^{3-33} acts as an antagonist on the GLP-2 receptor.

Body Weight and Small Intestinal Weight in Fasted and Re-fed Mice

Mice fasted for 24 hours exhibited a significant 14% ± 1% decrease in body weight ($P < .001$, fasting vs fed) (Table 3), whereas refeeding for a subsequent 24 hours completely restored weight back to fed levels ($P <$

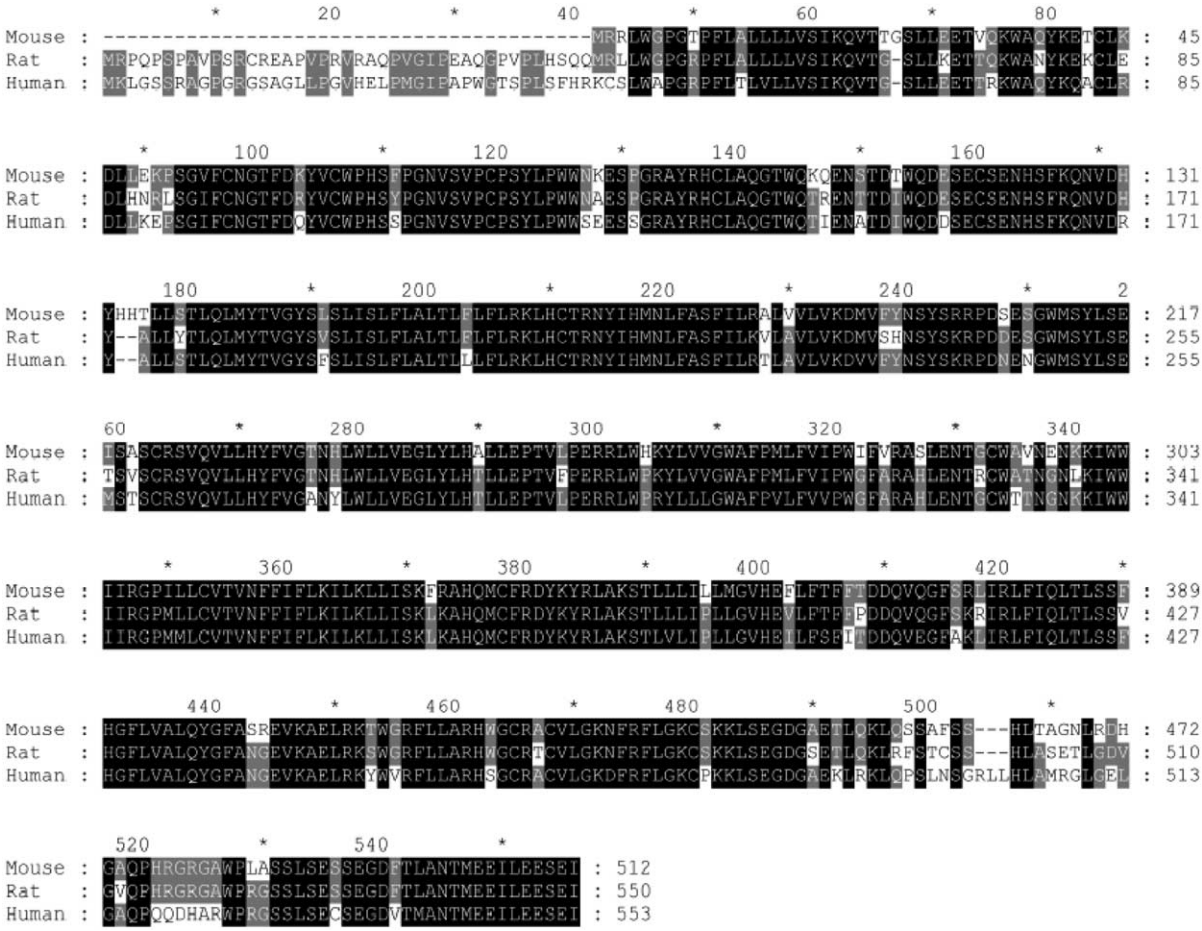

Figure 1. Multiple sequence alignment of the mouse, rat, and human GLP-2R amino acid sequences. Alignment was performed with CLUSTAL W[60] (1.82) and rendered with GENEDOC (version 2.6.002).[61] Identity between 2 of the 3 sequences is shown in *gray*, whereas *black shading* represents identity across all 3 receptor members. The GenBank accession number for the cloned mouse GLP-2R nucleotide sequence is AY605231.

.001 vs fasted, $P > .05$ vs fed). Small intestinal weight also decreased significantly, by 37% ± 1%, with fasting ($P < .001$ vs fed), and fully returned to fed levels with refeeding ($P < .001$ vs fasted, $P > .05$ vs fed) (Table 3). To assess whether these changes in intestinal weight were independent of the changes in body weight, small intestinal weights also were normalized to body weights. Fasting significantly decreased small intestinal weight relative to body weight, by 13% ± 2% ($P < .001$ vs fed), and refeeding completely restored relative small intestinal weight ($P < .001$ vs fasted, $P > .05$ vs fed) (Figure 3*A*).

To investigate the role of endogenous GLP-2 in the adaptive restoration of small intestinal weight, re-fed mice were treated concurrently with rGLP-$2^{3–33}$. Lower doses of rGLP-$2^{3–33}$ (.3 and 1 ng) did not affect relative small intestinal weight in re-fed mice (data not shown). However, administration of 3 ng of rGLP-$2^{3–33}$ significantly abrogated (by 55% ± 20%, $P < .05$) the recovery of small intestinal weight with refeeding, whereas 30 ng rGLP-$2^{3–33}$ completely (93% ± 27%, $P < .01$) prevented intestinal regrowth after refeeding. Furthermore, administration of 3 or 30 ng of rGLP-$2^{3–33}$ to control fed mice also resulted in a 12% ± 2% and 9% ± 2% reduction in relative small intestinal weight, respectively ($P < .001$ and $P < .01$ vs fed) (Figure 3*A*). In contrast to the effects on intestinal weight, treatment with rGLP-$2^{3–33}$ had no effect on body weight in either fed or re-fed mice (data not shown).

To determine whether the antagonistic effects of N-terminally truncated GLP-2 peptides are restricted to the specific rat isoform (rGLP-$2^{3–33}$), we also studied the effects of hGLP-$2^{3–33}$ after administration to re-fed mice. Consistent with observations made with rGLP-$2^{3–33}$ (Figure 3*A*), 3 and 30 ng of hGLP-$2^{3–33}$ partially (47% ± 43%, $P > .05$) and completely (103% ± 15%, $P < .05$) suppressed the restoration of relative small intestinal weight in re-fed mice (Figure 3*B*). Finally, to examine the specificity of the effects of GLP-$2^{3–33}$, several control peptides also were administered to the mice. The N-

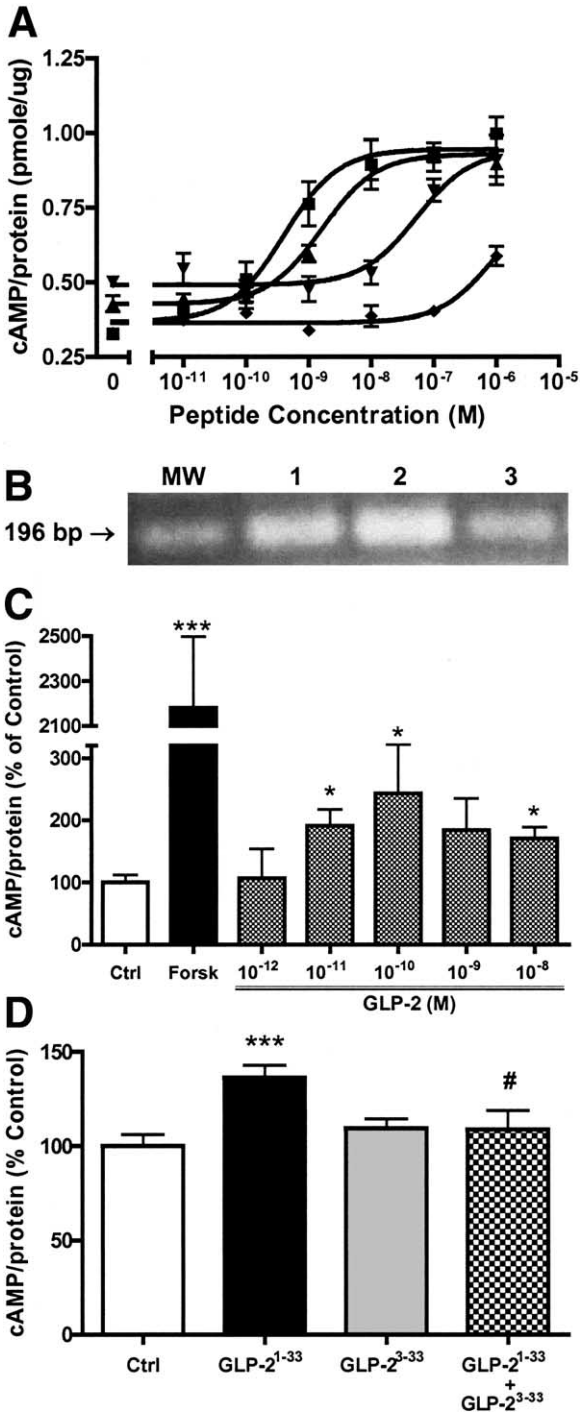

Figure 2. cAMP production by BHK-mGLP-2R cells and ex vivo murine intestinal muscle strips. (*A*) cAMP in BHK-mGLP-2R cells in response to h(Gly^2)-GLP-2 and/or rGLP-2$^{3–33}$. ■, h(Gly^2)-GLP-2 alone; h(Gly^2)-GLP-2 at indicated doses plus ▲, 100 nmol/L, or ▼, 1000 nmol/L rGLP-2$^{3–33}$; ♦, rGLP-2$^{3–33}$ alone (n = 3 per group). (*B*) RT-PCR for GLP-2 mRNA transcripts in 3 separate preparations of isolated mouse small intestinal muscle strips. The expected transcript size of 196 bp is indicated by the arrow (MW, 200-bp band of molecular weight ladder). (*C*) cAMP in murine intestinal muscle strips in response to vehicle, 100 μmol/L forskolin, or various doses of h(Gly^2)-GLP-2. (*D*) cAMP in murine intestinal muscle strips in response to GLP-2$^{1–33}$ (10^{-10} mol/L), GLP-2$^{3–33}$ (10^{-8} mol/L), or GLP-2$^{1–33}$ (10^{-10} mol/L) plus GLP-2$^{3–33}$ (10^{-8} mol/L). *$P < .05$, ***$P < .001$ vs control (CTRL); #$P < .05$ vs GLP-2$^{1–33}$ (10^{-10} mol/L) (n = 3–19 per group).

Table 3. Body and Small Intestinal Weight of Mice

	Fed	Fasted	Refed
Body weight (*g*)	23.5 ± .2	20.3 ± .4[a]	23.3 ± .4[b]
Small intestinal weight (*g*)	1.12 ± .02	.85 ± .01[a]	1.13 ± .03[b]

NOTE. Data are expressed as mean ± SEM. n = 13–29 per group, results are pooled from multiple independent experiments.
[a]$P < .001$ vs fed mice.
[b]$P < .001$ vs fasted mice.

terminally truncated peptide, GLP-2$^{5–33}$ (30 ng), reduced the adaptive regrowth seen in refeeding mice ($P < .05$), although the effectiveness of this peptide was less than that with the same dose of GLP-2$^{3–33}$ ($P < .001$; Figure 3*C*). In contrast, neither the structurally related peptide, GLP-1$^{7–36NH2}$ (30 ng) nor a molar equivalent dose of rat albumin (660 ng) had any effect on the small intestinal adaptive regrowth.

Food and Water Intake

To ascertain whether the effects of rGLP-2$^{3–33}$ on the small intestine of re-fed mice were independent of changes in satiety or thirst, food and water intake were measured in parallel experiments. Control fed mice consumed 4.6 ± .2 g/24 h of chow and re-fed mice consumed 5.9 ± .03 g/24 h of chow ($P > .05$). There was no effect of rGLP-2$^{3–33}$ on food intake in re-fed mice ($P > .05$). Fasting significantly increased water consumption from 5.2 ± .5 mL to 13.7 ± 3.3 mL ($P < .001$) and refeeding decreased water consumption back to fed levels ($P > .05$ vs fed). rGLP-2$^{3–33}$ treatment of refeeding mice did not affect water consumption ($P > .05$).

Crypt-Villus Heights

To understand the compartmental changes in the mucosal epithelium associated with fasting and refeeding, we examined jejunal crypt-villus height under different experimental conditions (Figure 4). Fasting significantly decreased crypt-villus height by 19% ± 2% ($P < .001$ vs fed), whereas crypt-villus height was restored to fed levels with refeeding ($P < .001$ vs fasted, $P > .05$ vs fed). The recovery of crypt-villus height in re-fed mice was reduced significantly by treatment with 3 or 30 ng of GLP-2$^{3–33}$, by 25% ± 20% and 32% ± 19%, respectively (both $P < .05$ vs re-fed). Furthermore, GLP-2$^{3–33}$ also produced an 8% ± 3% reduction in crypt-villus height in control fed mice (Figure 4*D*; $P < .05$ vs fed).

Small Intestinal Composition

Intestinal composition was examined to address the potential contributions of water and protein accretion/loss to the weight changes observed in the small

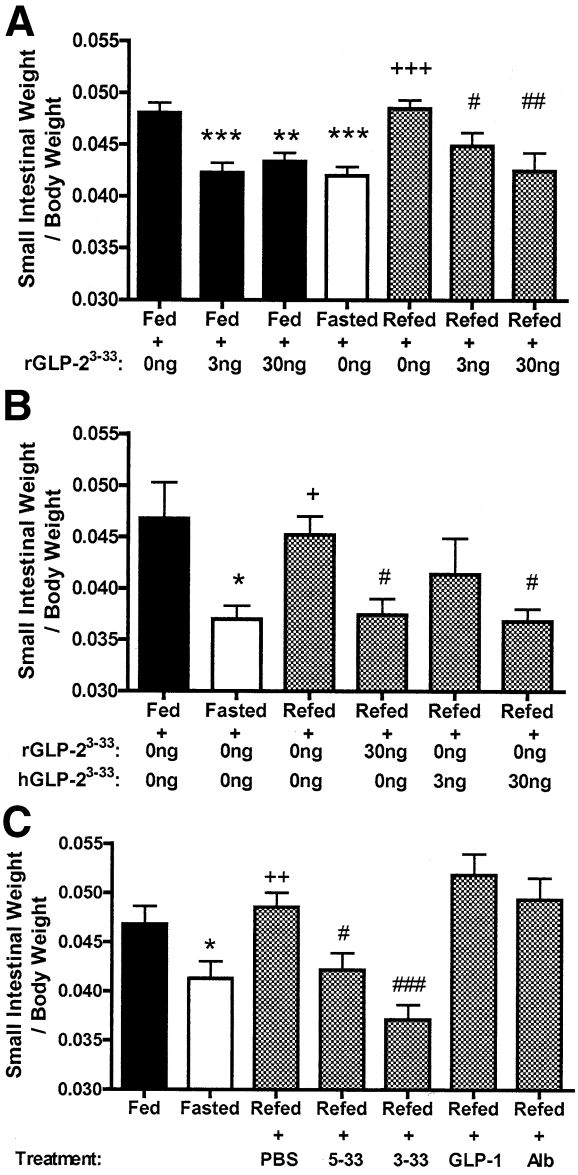

Figure 3. Relative small intestinal weight in control fed, fasting, or re-fed mice, with or without concurrent GLP-2[3–33] treatment. (*A*) Control fed, fasted, and re-fed mice were treated subcutaneously with vehicle alone (PBS) or with .3 or 30 ng of rGLP-2[3–33] twice a day (n = 13–28 per group, results are pooled from multiple independent experiments). (*B*) Control fed, fasted, and re-fed mice were treated subcutaneously with vehicle alone or with hGLP-2[3–33] twice a day (n = 4–6 per group, results are from a single independent experiment). (*C*) Control fed, fasted, and re-fed mice were treated subcutaneously with vehicle alone or with rGLP-2[5–33] (30 ng; 5–33), rGLP-2[3–33] (30 ng; 3–33), GLP-1[7–36NH2] (30 ng; GLP-1), or rat albumin (660 ng; molar equivalent to 30 ng of rGLP-2[5–33]; Alb) twice a day (n = 4–11 per group). $*P < .05$; $**P < .01$; $***P < .001$ vs control fed mice; $+P < .05$; $++P < .01$; $+++P < .001$ vs fasted mice; $\#P < .05$; $\#\#P < .01$; $\#\#\#P < .001$ vs re-fed mice.

intestine. The small intestine of fed mice was composed of 62% ± 1% water and 16% ± 1% protein, and the relative composition was not altered by fasting, refeeding, and/or treatment with rGLP-2[3–33] (data not shown).

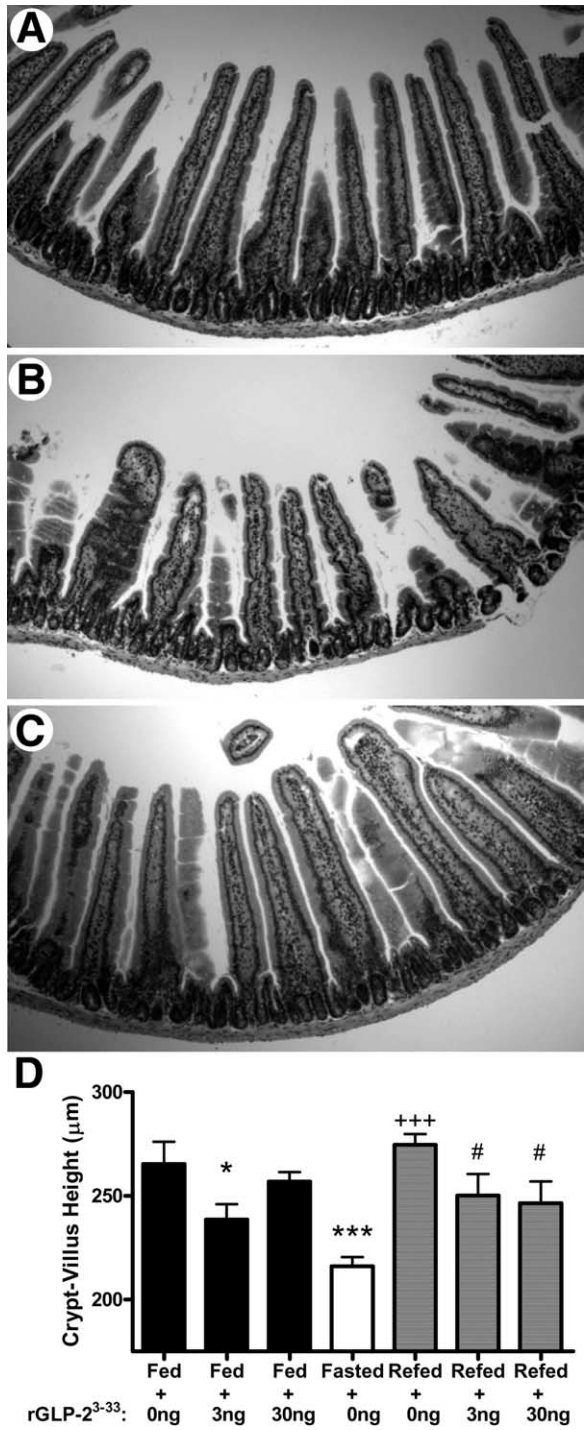

Figure 4. Morphometric analysis of control fed, fasted, and re-fed mice treated with or without rGLP-2[3–33]. (*A–C*) Representative histologic photographs of H&E-stained cross-section of the proximal jejunum of (*A*) control fed, (*B*) fasted, and (*C*) re-fed mice. Original magnification 10×. (*D*) Mean crypt-villus heights of control fed, fasted, and re-fed mice treated with or without rGLP-2[3–33] (for each mouse the mean of all measurements was made in 4 cross-sections, with an average of 28 measurements made per mouse) (n = 7–12 per group). $*P < .05$; $***P < .001$ vs control fed mice; $+++P < .001$ vs fasted mice; $\#P < .05$ vs re-fed mice.

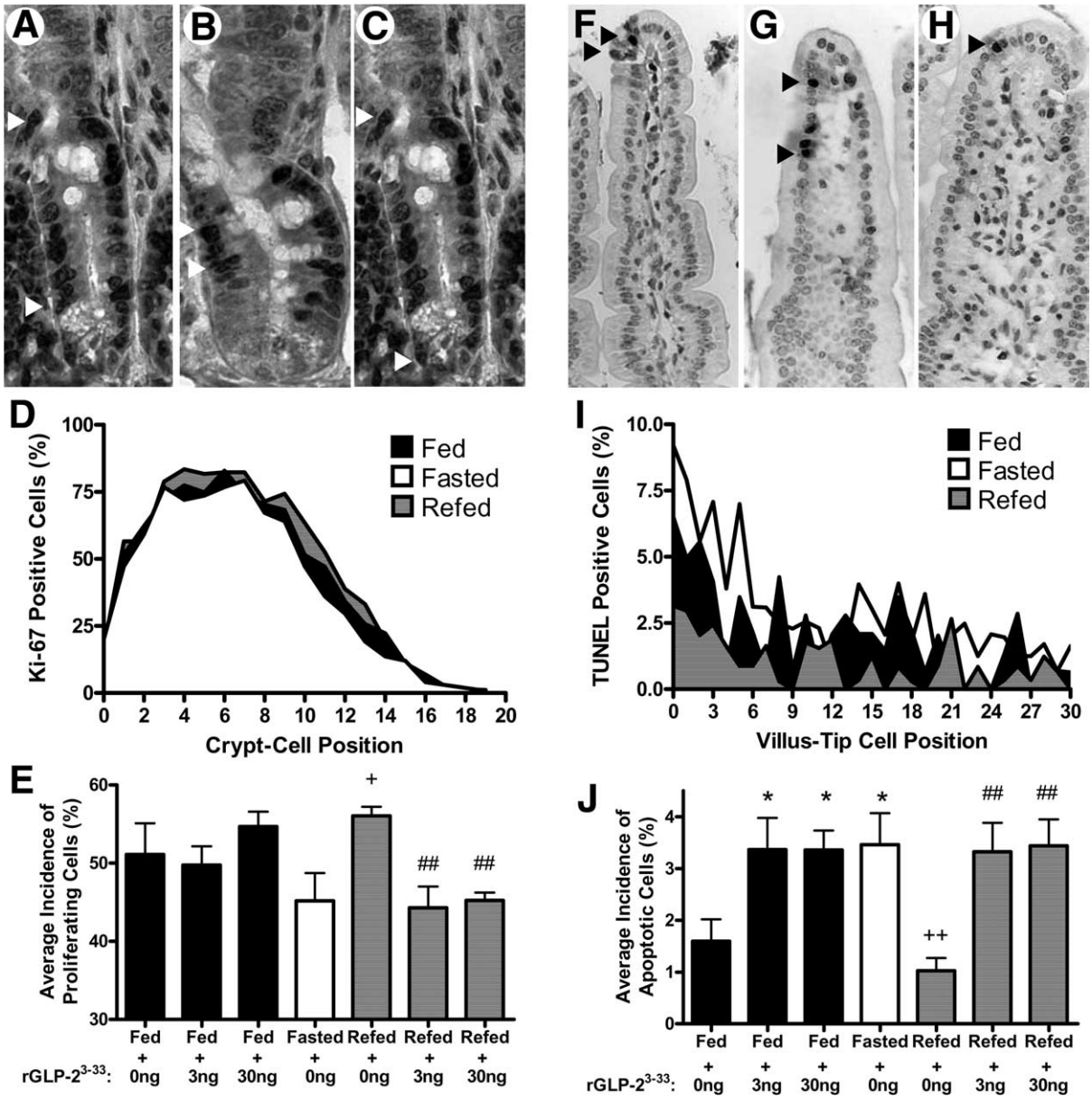

Figure 5. Crypt proliferation and villus apoptosis of control fed, fasted, and re-fed mice treated with or without rGLP-2[3–33]. (*A–E*) Crypt proliferation as determined by staining for Ki-67–immunopositive cells. (*A–C*) Representative Ki-67 staining (dark brown nuclei) in (*A*) control fed, (*B*) fasted, and (*C*) re-fed murine crypts. (*D*) Crypt proliferation index for control fed, fasted, and re-fed mice for each cell position along the crypt axis (position 0 denotes the crypt base). For each mouse, 25 crypts were analyzed, for n = 4–7 mice per group. Error bars were omitted for clarity. (*E*) Average incidence of crypt cell proliferation between cell positions 5–15 (inclusive) of control fed, fasted, and re-fed mice treated with or without rGLP-2[3–33]. (*F–J*) Villus apoptosis as determined by staining for TUNEL-immunopositive cells. (*F–H*) Representative TUNEL staining (dark brown nuclei) of control (*F*) fed, (*G*) fasted, and (*H*) re-fed murine villi. (*I*) Villus apoptosis for control fed, fasted, and re-fed mice for each cell position along the villus axis (position 0 denotes the villus tip). For each mouse 29–50 villus tips were analyzed, for n = 4–7 mice per group. Error bars were omitted for clarity. (*J*) Average incidence of villus apoptosis of control fed, fasted, and re-fed mice treated with or without rGLP-2[3–33]. (*D, I*) ■, Fed; □, fasted; ▩, re-fed. *$P < .05$ vs control fed mice; +$P < .05$; ++$P < .01$ vs fasted mice; ##$P < .01$ vs re-fed mice.

Apoptosis and Proliferation in the Murine Intestine After Fasting and Refeeding

To elucidate the mechanism(s) by which changes in enteral nutrients and endogenous GLP-2 activity affected small intestinal growth, enterocyte proliferation and apoptosis were examined along the crypt-villus axis in the presence or absence of GLP-2[3–33] (Figure 5). Cell proliferation, as assessed by the percentage of Ki-67–immunopositive cells, was observed almost exclusively in the crypts, with the greatest number of cells detected within the rapid proliferating transit zone (cell positions 5–15; Figure 5*A–D*).[36] The number of Ki-67–immunopositive cells was not decreased significantly with fasting but was increased significantly in re-fed mice, by

24% ± 3% ($P < .05$ vs fasted, $P > .05$ vs fed, Figure 5*E*). Administration of 3 or 30 ng of GLP-$2^{3–33}$ to re-fed mice completely prevented (by 108% ± 25% and 99% ± 9%, respectively) the increase in numbers of Ki-67–immunopositive cells (both $P < .01$ vs re-fed), but had no effect on the numbers of immunopositive cells in control fed mice ($P > .05$).

Apoptotic TUNEL-positive cells were observed along the entire villus; however, the highest occurrence was observed at the villus tip (Figure 5*F–I*). Villus-tip apoptosis increased by 99% ± 35% with fasting ($P < .05$ vs fed), whereas the number of TUNEL-positive cells decreased by 70% ± 7% with refeeding ($P < .05$ vs fasted, $P > .05$ vs fed, Figure 5*J*). Treatment with 3 or 30 ng of GLP-$2^{3–33}$ completely (99% ± 21% and 95% ± 23%, respectively) blocked the decrease in numbers of apoptotic cells observed in re-fed mice (both $P < .01$ vs re-fed). Furthermore, control fed mice treated with 3 or 30 ng of GLP-$2^{3–33}$ also exhibited a 93% ± 22% and 94% ± 35% increase in the number of apoptotic cells in the villus tips, respectively ($P < .05$ vs fed).

Small Intestinal Enzymatic Activities After Fasting and Refeeding

To determine the effects of nutrients and rGLP-$2^{3–33}$ on small intestinal digestive function, maltase, sucrase, and DP-IV enzymatic activities were examined. The relative activities of these enzymes in control fed mice were 87.6 ± .7, 9.5 ± .1, and 170.3 ± 8.4 U/g of protein, respectively, and these activities did not change with fasting, refeeding, or after administration of GLP-$2^{3–33}$ (data not shown).

Proglucagon and GLP-2–Receptor mRNA Transcripts After Fasting and Refeeding

To ascertain whether the major components of the GLP-2–GLP-2R axis were regulated by refeeding and/or rGLP-$2^{3–33}$, mRNA transcript levels for proglucagon and the GLP-2R were determined by semiquantitative RT-PCR using RNA prepared from the ileum and jejunum, respectively (Figure 6). Fasting decreased the levels of proglucagon mRNA transcripts by 72% ± 7% ($P < .01$ vs fed), whereas proglucagon mRNA transcripts were increased by 356% ± 94% with refeeding (Figure 6*A*; $P < .001$ vs fasted, $P > .05$ vs fed). GLP-$2^{3–33}$ had no effect on the levels of proglucagon mRNA transcripts. In contrast, fasting and refeeding had no effect on GLP-2R mRNA transcript levels. GLP-$2^{3–33}$ reduced the levels of GLP-2R mRNA transcripts in control fed mice (by 76% ± 11%, $P < .05$ vs fed), but not in fasted/re-fed mice (Figure 6*B*).

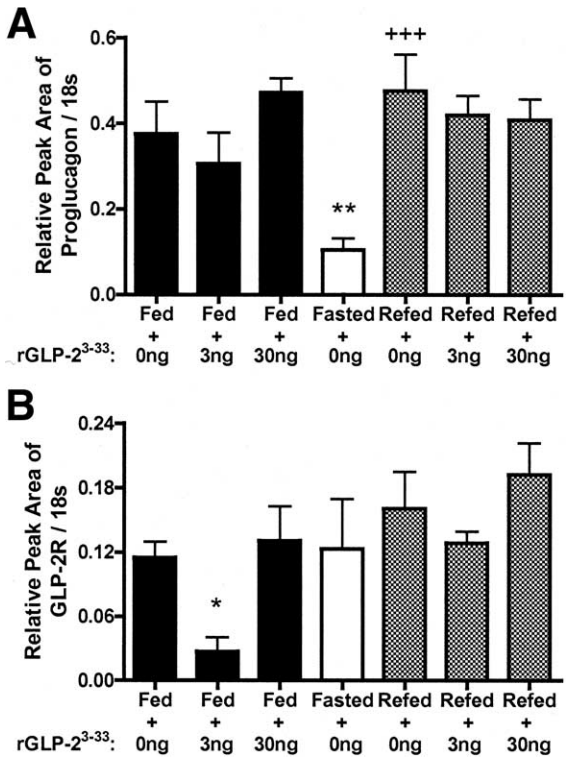

Figure 6. Semiquantitative RT-PCR analysis for proglucagon and GLP-2R mRNA transcript levels in control fed, fasted, and re-fed mice treated with or without rGLP-$2^{3–33}$. (*A*) Relative levels of ileal proglucagon mRNA transcripts, and (*B*) relative levels of jejunal GLP-2R mRNA transcripts, as determined by peak area after ultraviolet HPLC analysis (n = 3–4 per group). *$P < .05$; **$P < .01$ vs control fed mice; +++$P < .001$ vs fasted mice.

Plasma Levels of GLP-2

To assess whether exogenous GLP-$2^{3–33}$ modulated plasma levels of endogenous GLP-$2^{1–33}$ in vivo, rat plasma was assayed for both GLP-$2^{1–33}$ and GLP-$2^{3–33}$ after subcutaneous administration of GLP-$2^{3–33}$ (Figure 7). Plasma GLP-$2^{1–33}$ levels did not change after GLP-$2^{3–33}$ injection relative to saline controls ($P > 0.05$). Furthermore, although circulating levels of GLP-$2^{3–33}$ were increased by 550% ± 235% ($P < .05$ vs saline controls), the plasma levels of GLP-$2^{3–33}$ achieved were similar to those of endogenous GLP-$2^{1–33}$. These findings therefore suggest that the biological actions of GLP-$2^{3–33}$ on intestinal weight in vivo are not mediated through suppression of endogenous circulating levels of GLP-$2^{1–33}$.

Discussion

Our current understanding of the intestinotropic actions of GLP-2 largely is based on studies in which the peptide was administered exogenously, thereby resulting in supraphysiologic levels of circulating peptide in either normal mice or in mice with pathologic disturbances in gut function. The results of the present study show that

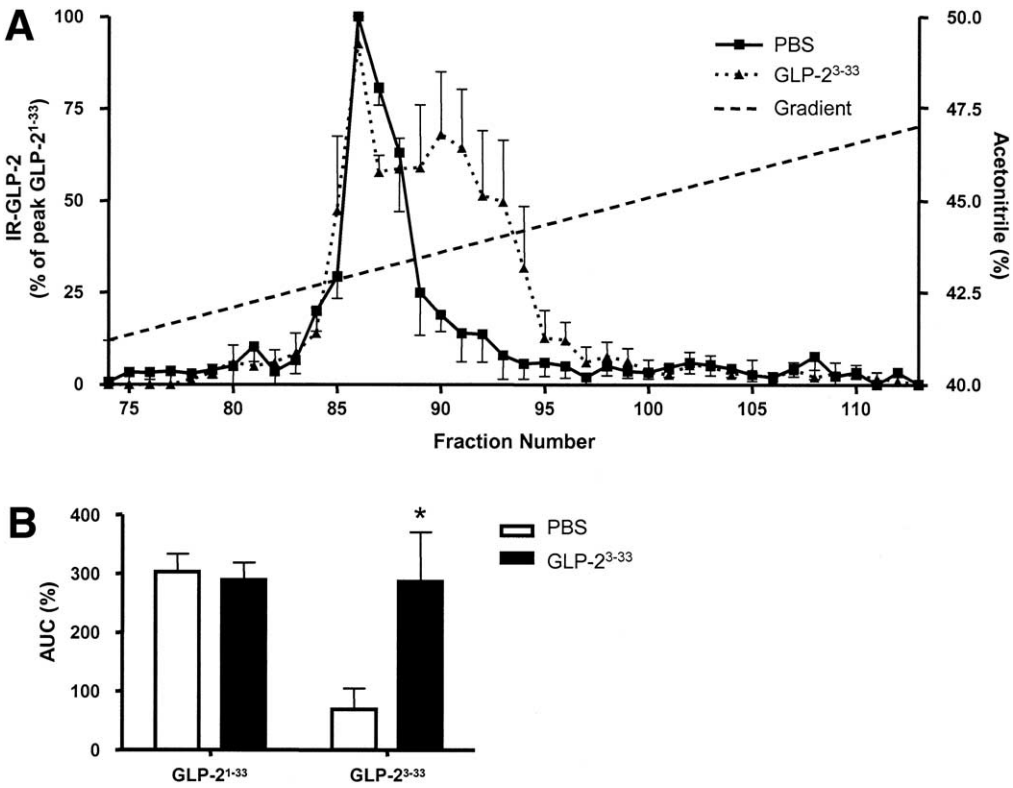

Figure 7. Plasma levels of GLP-$2^{1–33}$ and GLP-$2^{3–33}$. (*A*) Plasma was collected from rats 30 minutes after subcutaneous injection of PBS or 1.2 μg/kg GLP-$2^{3–33}$ and HPLC fractions were collected and analyzed by radioimmunoassay (n = 3). Synthetic GLP-$2^{1–33}$ and GLP-$2^{3–33}$ eluted at fractions 86 and 90, respectively. ■, PBS; ▲, GLP-$2^{3–33}$; ---, gradient. (*B*) Area-under-the-curve (AUC) analysis of the GLP-$2^{1–33}$ (fractions 82–88) and GLP-$2^{3–33}$ (fractions 88–94) profiles in (*A*). (*B*) □, PBS; ■, GLP-$2^{3–33}$. $*P < .05$ vs PBS control.

endogenous GLP-2 is a physiologic regulator of the intestinotropic response to refeeding in normal mice.

In our current model of gut adaptation, mice that were fasted for 24 hours and then subsequently re-fed for 24 hours showed an acute atrophy of the gut followed by physiologic regrowth back to normal levels, consistent with the results of previous studies.[1,2] By using GLP-$2^{3–33}$ as a GLP-2R antagonist, we have now shown that endogenous GLP-2 facilitates this restoration of gut structure in re-fed mice via elongation of the crypt-villus axis. Furthermore, endogenous GLP-2 also was shown to play a role in the maintenance of normal gut structure in control fed mice. These effects were observed using both rat and human GLP-$2^{3–33}$ as GLP-2R antagonists, and also were seen to a lesser extent with the shorter fragment GLP-$2^{5–33}$, but not with either GLP-$1^{7–36NH2}$ or rat albumin. The reduction in crypt-villus height observed in fasted mice is consistent with the associated reductions in the circulating levels of GLP-2 that occur with the loss of luminal nutrients in the fasted state.[9,10,22,37] These findings also are consistent with the demonstration that administration of GLP-2 prevents the gut atrophy associated with total parenteral nutrition in rats and pigs.[38,39] Similarly, studies of GLP-2 immunoneutralization in the rat have suggested a role for GLP-2 in the intestinal growth associated with streptozotocin-induced, insulin-deficient, hyperphagic diabetes.[40] Our study extends these findings by showing a physiologic role for endogenous GLP-2 in the nutrient-dependent regulation of intestinal growth.

Investigation of the mechanism by which endogenous GLP-2 regulates the growth of the crypt-villus axis showed a clear correlation of GLP-2–mediated changes in small intestinal growth with alterations in both crypt cell proliferation and villus cell apoptosis. Interestingly, GLP-2–stimulated proliferation in re-fed mice was found to occur in the rapidly dividing transit cell region (cells 5–15), a subset of undifferentiated cells believed to be responsible for expansion of the stem cell population that resides immediately below this region.[36] Previous studies showing stimulatory effects of exogenous GLP-2 on crypt-cell proliferation in rodents have not reported on the distribution of the proliferating cells within the crypts.[7,41–43] However, Dahly et al[44] found that insulin-like growth factor-1 enhances proliferation in both the mid- (cells 11–20) and upper- (cells 21–30) crypt in rats on total parenteral nutrition after massive small-bowel resection. In contrast, keratinocyte growth factor stimulates proliferation in cell positions 1–7 in murine crypts, but decreases mitotic labeling in cells at positions 9–15,[29] while transforming growth factor β3 inhibits proliferation in cell positions 3–4 and 13–27.[45] Thus, the actions of GLP-2, at least in re-fed mice, appear to be

localized to a distinct region relative to observations made with other intestinal growth factors.

Notably, 24 hours of fasting induced a 2-fold increase in villus apoptosis, and this was reversed by 70% in re-fed mice. Administration of GLP-2^{3-33} prevented this reversal. The regulation of apoptosis is well established to be a key mechanism regulating gut growth during fasting and refeeding,[46–49] and our data suggest that endogenous GLP-2 is a physiologically relevant component of this adaptive process. Several studies have reported on the distribution of apoptotic cells along the villus in response to exogenous GLP-2 administration; however, the majority of these experiments used gut injury models, such as intestinal inflammation, chemotherapy-induced intestinal mucositis, and short-bowel resection with total parenteral nutrition.[12–14,42,50] Consistent with our findings, the incidence of apoptosis in the normal intestine, as detected by the TUNEL assay, appears to be highest at the villus tip.[7,46,49]

A number of control experiments were performed to ensure that the changes observed in intestinal weight in response to GLP-2^{3-33} were specific to the effects of GLP-2 on the intestine. GLP-2^{3-33} had no effect on food or water intake, and it did not change intestinal composition. A recent study by Tang-Christensen et al[51] showed that GLP-2 can inhibit food intake when injected into the brain of rats. However, peripheral administration of GLP-2^{3-33} had no effect on intake of either food or water in the present study, and no changes in body weight were observed. Furthermore, no change in the protein or water composition of the small intestine was found in response to nutritional status or GLP-2^{3-33} treatment. Finally, exogenous GLP-2^{3-33} did not suppress the circulating levels of GLP-2^{1-33}. Hence, the available evidence suggests that GLP-2^{3-33} exerted its effects via attenuation of the actions of endogenous GLP-2, likely mediated through effects on proliferation and apoptosis, leading to changes in crypt-villus height.

Previous studies using GLP-2^{3-33} have shown either no effect,[25,52] weak agonist activity,[26,52] or an antagonistic effect[26] of GLP-2^{3-33} when co-administered with supraphysiologic levels of GLP-2^{1-33} or h(Gly^2)-GLP-2^{1-33}. These diverse findings are likely a result of differences in the species used (eg, mice and rats), duration of treatment, and the specific doses of GLP-2^{3-33} administered in the various experiments. Our in vitro studies and a parallel study by Thulesen et al[26] have shown GLP-2^{3-33} to be a partial agonist for the GLP-2 receptor at higher concentrations in vitro. Thus, doses of GLP-2^{3-33} must be selected carefully to elicit a preferential antagonistic response at the GLP-2 receptor. Hence, studies in which GLP-2^{3-33} was shown to exert a partial agonist response used 100- to 1000-fold higher amounts of peptide as compared with the concentrations administered in the present study.[26,52] Thus, somewhat paradoxically, to antagonize the effects of endogenous GLP-2, low doses of GLP-2^{3-33} must be administered. Furthermore, in addition to the present findings with both the BHK-mGLP-R cells and the ex vivo muscle strips, a number of in vitro studies have provided evidence for an antagonistic effect of GLP-2^{3-33} on the GLP-2R. Structure-function studies have shown the N-terminus of GLP-2 and amino acids 1–3 in particular are critical for receptor activation but not for receptor binding.[28] Furthermore, receptor-binding studies have shown GLP-2^{3-33} to possess comparable binding affinity to the full-length ligand GLP-2^{1-33}.[25,26] Taken together, these studies suggest that GLP-2^{3-33} retains the capacity to bind to its receptor but exhibits a reduced capacity for receptor activation owing to truncation of the crucial N-terminal bioactive domain.

Further support for the antagonistic response of the DP-IV metabolite of GLP-2 can be ascertained from parallel studies on hormones of the related glucagon peptide superfamily.[53] The peptides within this family share considerable sequence homology, and many are inactivated by DP-IV cleavage.[54] Furthermore, GLP-$1^{9-36amide}$ antagonizes the effects of intact GLP-$1^{7-36amide}$ both in vitro and in vivo.[55,56] Moreover, Gault et al[57] showed that the DP-IV metabolite, GIP^{3-42} inhibits the actions of GIP^{1-42}. Hence, N-terminally truncated DP-IV metabolites, including GLP-2^{3-33}, commonly display antagonistic properties at their respective cognate receptors.

Sequence analysis of the murine GLP-2R showed 85%–90% amino acid identity with the human and rat GLP-2R, respectively. Previous studies have shown that there is no difference between h(Gly^2)-GLP-2^{1-33} and rGLP-2^{1-33} in their ability to stimulate the GLP-2R, with an EC_{50} of .04–14 nmol/L reported for both peptides with the human and rat GLP-2R.[25,26,28,33,34,58] Consistent with these reports, we found an EC_{50} of ~.4 nmol/L for the mGLP-2R using h(Gly^2)-GLP-2^{1-33}. These findings suggest strong similarities in the response of the 3 different (murine, rat, and human) GLP-2 receptors to GLP-2R agonists. The minor variances in responsiveness obtained with the different receptors likely can be explained largely by potential differences in the density of receptor expression in the cell lines used.[59]

In summary, the findings of the present study provide evidence for an essential role of GLP-2 in maintaining intestinal structure in the fed state, as well as during adaptation in response to nutrient deprivation and sub-

sequent refeeding. Because no model of GLP-2 or GLP-2R deficiency is available, the characterization of GLP-2[3–33] as a GLP-2R antagonist provides a useful experimental reagent by which the physiologic roles of GLP-2 may be explored in other models of intestinal growth or insufficiency.

References

1. Nian M, Gu J, Irwin DM, Drucker DJ. Human glucagon gene promoter sequences regulating tissue-specific versus nutrient-regulated gene expression. Am J Physiol 2002;282:R173–R183.
2. Goodlad RA, Wright NA. The effects of starvation and refeeding on intestinal cell proliferation in the mouse. Virchows Arch 1984;45: 63–73.
3. Jeejeebhoy KN. Total parenteral nutrition: potion or poison? Am J Clin Nutr 2001;74:160–163.
4. Buchman AL, Moukarzel AA, Bhuta S, Belle M, Ament ME, Eckhert CD, Hollander D, Gornbein J, Kopple JD, Vijayaroghavan SR. Parenteral nutrition is associated with intestinal morphologic and functional changes in humans. J Parenter Enteral Nutr 1995;19: 453–460.
5. Botsios DS, Vasiliadis KD. Factors enhancing intestinal adaptation after bowel compensation. Dig Dis 2003;21:228–236.
6. Drucker DJ, Erlich P, Asa SL, Brubaker PL. Induction of intestinal epithelial proliferation by glucagon-like peptide 2. Proc Natl Acad Sci U S A 1996;93:7911–7916.
7. Tsai CH, Hill M, Asa SL, Brubaker PL, Drucker DJ. Intestinal growth-promoting properties of glucagon-like peptide-2 in mice. Am J Physiol 1997;273:E77–E84.
8. Eissele R, Goke R, Willemer S, Harthus HP, Vermeer H, Arnold R, Goke B. Glucagon-like peptide-1 cells in the gastrointestinal tract and pancreas of rat, pig and man. Eur J Clin Invest 1992;22: 283–291.
9. Orskov C, Holst JJ, Knuhtsen S, Baldissera FG, Poulsen SS, Nielsen OV. Glucagon-like peptides GLP-1 and GLP-2, predicted products of the glucagon gene, are secreted separately from pig small intestine but not pancreas. Endocrinology 1986;119: 1467–1475.
10. Xiao Q, Boushey RP, Drucker DJ, Brubaker PL. Secretion of the intestinotropic hormone glucagon-like peptide 2 is differentially regulated by nutrients in humans. Gastroenterology 1999;117: 99–105.
11. L'Heureux MC, Brubaker PL. Glucagon-like peptide-2 and common therapeutics in a murine model of ulcerative colitis. J Pharmacol Exp Ther 2003;306:347–354.
12. Drucker DJ, Yusta B, Boushey RP, DeForest L, Brubaker PL. Human [Gly2]GLP-2 reduces the severity of colonic injury in a murine model of experimental colitis. Am J Physiol 1999;276: G79–G91.
13. Boushey RP, Yusta B, Drucker DJ. Glucagon-like peptide (GLP)-2 reduces chemotherapy-associated mortality and enhances cell survival in cells expressing a transfected GLP-2 receptor. Cancer Res 2001;61:687–693.
14. Boushey RP, Yusta B, Drucker DJ. Glucagon-like peptide 2 decreases mortality and reduces the severity of indomethacin-induced murine enteritis. Am J Physiol 1999;277:E937–E947.
15. Brubaker PL, Izzo A, Hill M, Drucker DJ. Intestinal function in mice with small bowel growth induced by glucagon-like peptide-2. Am J Physiol 1997;272:E1050–E1058.
16. Cheeseman CI. Upregulation of SGLT-1 transport activity in rat jejunum induced by GLP-2 infusion in vivo. Am J Physiol 1997; 273:R1965–R1971.
17. Kato Y, Yu D, Schwartz MZ. Glucagonlike peptide-2 enhances small intestinal absorptive function and mucosal mass in vivo. J Pediatr Surg 1999;34:18–20.
18. Benjamin MA, McKay DM, Yang PC, Cameron H, Perdue MH. Glucagon-like peptide-2 enhances intestinal epithelial barrier function of both transcellular and paracellular pathways in the mouse. Gut 2000;47:112–119.
19. Wojdemann M, Wettergren A, Hartmann B, Holst JJ. Glucagon-like peptide-2 inhibits centrally induced antral motility in pigs. Scand J Gastroenterol 1998;33:828–832.
20. Jeppesen PB, Hartmann B, Thulesen J, Graff J, Lohmann J, Hansen BS, Tofteng F, Poulsen SS, Madsen JL, Holst JJ, Mortensen PB. Glucagon-like peptide 2 improves nutrient absorption and nutritional status in short-bowel patients with no colon. Gastroenterology 2001;120:806–815.
21. Brubaker PL, Crivici A, Izzo A, Ehrlich P, Tsai CH, Drucker DJ. Circulating and tissue forms of the intestinal growth factor, glucagon-like peptide-2. Endocrinology 1997;138:4837–4843.
22. Hartmann B, Harr MB, Jeppesen PB, Wojdemann M, Deacon CF, Mortensen PB, Holst JJ. In vivo and in vitro degradation of glucagon-like peptide-2 in humans. J Clin Endocrinol Metab 2000;85: 2884–2888.
23. Tavares W, Drucker DJ, Brubaker PL. Enzymatic- and renal-dependent catabolism of the intestinotropic hormone glucagon-like peptide-2 in rats. Am J Physiol 2000;278:E134–E139.
24. Drucker DJ, Shi Q, Crivici A, Sumner-Smith M, Tavares W, Hill M, DeForest L, Cooper S, Brubaker PL. Regulation of the biological activity of glucagon-like peptide 2 in vivo by dipeptidyl peptidase IV. Nat Biotechnol 1997;15:673–677.
25. Munroe DG, Gupta AK, Kooshesh F, Vyas TB, Rizkalla G, Wang H, Demchyshyn L, Yang ZJ, Kamboj RK, Chen H, McCallum K, Sumner-Smith M, Drucker DJ, Crivici A. Prototypic G protein-coupled receptor for the intestinotrophic factor glucagon-like peptide 2. Proc Natl Acad Sci U S A 1999;96:1569–1573.
26. Thulesen J, Knudsen LB, Hartmann B, Hastrup S, Kissow H, Jeppesen PB, Orskov C, Holst JJ, Poulsen SS. The truncated metabolite GLP-2 (3-33) interacts with the GLP-2 receptor as a partial agonist. Regul Pept 2002;103:9–15.
27. Yusta B, Huang L, Munroe D, Wolff G, Fantaske R, Sharma S, Demchyshyn L, Asa SL, Drucker DJ. Enteroendocrine localization of GLP-2 receptor expression in humans and rodents. Gastroenterology 2000;119:744–755.
28. DaCambra MP, Yusta B, Sumner-Smith M, Crivici A, Drucker DJ, Brubaker PL. Structural determinants for activity of glucagon-like peptide-2. Biochemistry 2000;39:8888–8894.
29. Potten CS, O'Shea JA, Farrell CL, Rex K, Booth C. The effects of repeated doses of keratinocyte growth factor on cell proliferation in the cellular hierarchy of the crypts of the murine small intestine. Cell Growth Differ 2001;12:265–275.
30. Bjerknes M, Cheng H. Modulation of specific intestinal epithelial progenitors by enteric neurons. Proc Natl Acad Sci U S A 2001; 98:12497–12502.
31. Selvey S, Thompson EW, Matthaei K, Lea RA, Irving MG, Griffiths LR. Beta-actin—an unsuitable internal control for RT-PCR. Mol Cell Probes 2001;15:307–311.
32. Hill ME, Asa SL, Drucker DJ. Essential requirement for Pax6 in control of enteroendocrine proglucagon gene transcription. Mol Endocrinol 1999;13:1474–1486.
33. Estall JL, Yusta B, Drucker DJ. Lipid raft-dependent GLP-2 receptor trafficking occurs independently of agonist-induced desensitization. Mol Biol Cell 2004;15:3673–3687.
34. Lovshin J, Estall J, Yusta B, Brown TJ, Drucker DJ. Glucagon-like peptide (GLP)-2 action in the murine central nervous system is enhanced by elimination of GLP-1 receptor signaling. J Biol Chem 2001;276:21489–21499.
35. Walsh NA, Yusta B, DaCambra MP, Anini Y, Drucker DJ, Brubaker PL. Glucagon-like peptide-2 receptor activation in the rat intestinal mucosa. Endocrinology 2003;144:4385–4392.
36. Marshman E, Booth C, Potten CS. The intestinal epithelial stem cell. Bioessays 2002;24:91–98.

37. van Goudoever JB, Stoll B, Hartmann B, Holst JJ, Reeds PJ, Burrin DG. Secretion of trophic gut peptides is not different in bolus- and continuously fed piglets. J Nutr 2001;131:729–732.
38. Chance WT, Foley-Nelson T, Thomas I, Balasubramaniam A. Prevention of parenteral nutrition-induced gut hypoplasia by coinfusion of glucagon-like peptide-2. Am J Physiol 1997;273:G559–G563.
39. Burrin DG, Stoll B, Jiang R, Petersen Y, Elnif J, Buddington RK, Schmidt M, Holst JJ, Hartmann B, Sangild PT. GLP-2 stimulates intestinal growth in premature TPN-fed pigs by suppressing proteolysis and apoptosis. Am J Physiol 2000;279:G1249–G1256.
40. Hartmann B, Thulesen J, Hare KJ, Kissow H, Orskov C, Poulsen SS, Holst JJ. Immunoneutralization of endogenous glucagon-like peptide-2 reduces adaptive intestinal growth in diabetic rats. Regul Pept 2002;105:173–179.
41. Drucker DJ, DeForest L, Brubaker PL. Intestinal response to growth factors administered alone or in combination with human [Gly2]glucagon-like peptide 2. Am J Physiol 1997;273:G1252–G1262.
42. Martin GR, Wallace LE, Sigalet DL. Glucagon-like peptide-2 induces intestinal adaptation in parenterally fed rats with short bowel syndrome. Am J Physiol 2004;286:G964–G972.
43. Ghatei MA, Goodlad RA, Taheri S, Mandir N, Brynes AE, Jordinson M, Bloom SR. Proglucagon-derived peptides in intestinal epithelial proliferation: glucagon-like peptide-2 is a major mediator of intestinal epithelial proliferation in rats. Dig Dis Sci 2001;46:1255–1263.
44. Dahly EM, Guo Z, Ney DM. IGF-I augments resection-induced mucosal hyperplasia by altering enterocyte kinetics. Am J Physiol 2003;285:R800–R808.
45. Booth D, Haley JD, Bruskin AM, Potten CS. Transforming growth factor-B3 protects murine small intestinal crypt stem cells and animal survival after irradiation, possibly by reducing stem-cell cycling. Int J Cancer 2000;86:53–59.
46. Chappell VL, Thompson MD, Jeschke MG, Chung DH, Thompson JC, Wolf SE. Effects of incremental starvation on gut mucosa. Dig Dis Sci 2003;48:765–769.
47. Holt PR, Moss SF, Heydari AR, Richardson A. Diet restriction increases apoptosis in the gut of aging rats. J Gerontol A Biol Sci Med Sci 1998;53:B168–B172.
48. Martins MJ, Hipolito-Reis C, Azevedo I. Effect of fasting on rat duodenal and jejunal microvilli. Clin Nutr 2001;20:325–331.
49. Boza JJ, Moennoz D, Vuichoud J, Jarret AR, Gaudard-de-Weck D, Fritsche R, Donnet A, Schiffrin EJ, Perruisseau G, Ballevre O. Food deprivation and refeeding influence growth, nutrient retention and functional recovery of rats. J Nutr 1999;129:1340–1346.
50. Dahly EM, Gillingham MB, Guo Z, Murali SG, Nelson DW, Holst JJ, Ney DM. Role of luminal nutrients and endogenous GLP-2 in intestinal adaptation to mid-small bowel resection. Am J Physiol 2003;284:G670–G682.
51. Tang-Christensen M, Larsen PJ, Thulesen J, Romer J, Vrang N. The proglucagon-derived peptide, glucagon-like peptide-2, is a neurotransmitter involved in the regulation of food intake. Nat Med 2000;6:802–807.
52. Hartmann B, Thulesen J, Kissow H, Thulesen S, Orskov C, Ropke C, Poulsen SS, Holst JJ. Dipeptidyl peptidase IV inhibition enhances the intestinotrophic effect of glucagon-like peptide-2 in rats and mice. Endocrinology 2000;141:4013–4020.
53. Sherwood NM, Krueckl SL, McRory JE. The origin and function of the pituitary adenylate cyclase-activating polypeptide (PACAP)/glucagon superfamily. Endocr Rev 2000;21:619–670.
54. Zhu L, Tamvakopoulos C, Xie D, Dragovic J, Shen X, Fenyk-Melody JE, Schmidt K, Bagchi A, Griffin PR, Thornberry NA, Sinha RR. The role of dipeptidyl peptidase IV in the cleavage of glucagon family peptides: in vivo metabolism of pituitary adenylate cyclase activating polypeptide-(1-38). J Biol Chem 2003;278:22418–22423.
55. Knudsen LB, Pridal L. Glucagon-like peptide-1-(9-36) amide is a major metabolite of glucagon-like peptide-1-(7-36) amide after in vivo administration to dogs, and it acts as an antagonist on the pancreatic receptor. Eur J Pharmacol 1996;318:429–435.
56. Gallwitz B, Schmidt WE, Conlon JM, Creutzfeldt W. Glucagon-like peptide-1(7-36)amide: characterization of the domain responsible for binding to its receptor on rat insulinoma RINm5F cells. J Mol Endocrinol 1990;5:33–39.
57. Gault VA, Parker JC, Harriott P, Flatt PR, O'Harte FP. Evidence that the major degradation product of glucose-dependent insulinotropic polypeptide, GIP(3-42), is a GIP receptor antagonist in vivo. J Endocrinol 2002;175:525–533.
58. Yusta B, Somwar R, Wang F, Munroe D, Grinstein S, Klip A, Drucker DJ. Identification of glucagon-like peptide-2 (GLP-2)-activated signaling pathways in baby hamster kidney fibroblasts expressing the rat GLP-2 receptor. J Biol Chem 1999;274:30459–30467.
59. Fehmann HC, Pracht A, Goke B. High-level expression of the GLP-1 receptor results in receptor desensitization. Pancreas 1998;17:309–314.
60. Chenna R, Sugawara H, Koike T, Lopez R, Gibson TJ, Higgins DG, Thompson JD. Multiple sequence alignment with the Clustal series of programs. Nucl Acids Res 2003;31:3497–3500.
61. Nicholas KB, Nicholas HB JR, Deerfield DW II. GeneDoc: analysis and visualization of genetic variation. EMBNEW.NEWS 1997;4:14.

Received June 28, 2004. Accepted February 2, 2005.

Address requests for reprints to: Patricia L. Brubaker, PhD, Room 3366 Medical Sciences Building, University of Toronto, 1 King's College Circle, Toronto, Ontario, M5S 1A8 Canada. e-mail: p.brubaker@utoronto.ca; fax: (416) 978-2593.

Supported by an Ontario Graduate Scholarship (to E.D.S.); by studentships from the Banting and Best Diabetes Centre-Novo Nordisk and by a Canada Graduate Scholarship Doctoral Award from the Canadian Institutes of Health Research (to J.L.E.); by the Canada Research Chairs Program (to P.L.B., D.J.D.); by operating grants from the Canadian Institutes of Health Research (to P.L.B., D.J.D.); and by a grant from the Ontario Research and Development Challenge Fund (to D.J.D.).

The authors are grateful to J. Yue (Department of Physiology, University of Toronto) for assistance with the rat cannulations, to Dr S. St-Pierre (Peptidec Technologies, Ltd., Pierrefonds, Quebec, Canada) for peptide synthesis, and to NPS-Allelix for the gift of peptide.